Electronic Supplementary Material (ESI) for New Journal of Chemistry.

Cocktail effect in high-entropy perovskite oxide for boosting alkaline oxygen evolution

Jiace Hao[a], Fengjun Ma[a], Yu Chen[a], Shuanglong Lu[a], Fang Duan[a], Mingliang Du*, Chenglong Wang[b*],
Wenchao Zhang[c], and Han Zhu[a*]

a Key Laboratory of Synthetic and Biological Colloids, Ministry of Education, School of Chemical and Material Engineering, Jiangnan University, Wuxi, Jiangsu 214122, P. R. China. E-mail: zhysw@jiangnan.edu.cn; du@jiangnan.edu.cn

b Engineering Research Center for Eco-Dyeing and Finishing of Textiles, Ministry of Education, Zhejiang Sci-Tech University, Hangzhou 310018, P. R. China. E-mail: wcl_charles@126.com

c School of Chemistry and Life Sciences, Suzhou University of Science and Technology, Suzhou, Jiangsu 215009, P. R. China.

Experimental

Materials

Lanthanum nitrate hexahydrate ($La(NO_3)_3·6H_2O$, 99%), strontium acetate ($(CH_3COO)_2Sr$, AR, 99.0%), iron nitrate nonahydrate ($Fe(NO_3)_2·6H_2O$, AR, 99.0%), cobalt nitrate hexahydrate ($Co(NO_3)_2·6H_2O$, AR, 99.99%), nickel nitrate hexahydrate ($Ni(NO_3)_2·6H_2O$, AR, 99.99%), cupric nitrate hexahydrate ($Cu(NO_3)_2·6H_2O$, AR, 99.99%), manganous acetate ($(CH_3COO)_2Mn$, AR, 99.0%), and Nafion117 solution (5 wt%) were acquired from Shanghai Aladdin Biochemical Technology Co., Ltd. Ethanol (C_2H_5OH,99.7%) and N,N-Dimethylformamide (DMF, AR, 99.5%) were purchased from Sinopharm Chemical Reagent Co. Polyvinylpyrrolidone (PVP, $M_w \approx 1300000$) was manufactured by energy chemical Co. Ltd. All of the chemicals were used without further purification. Deionized water (DIW, 18.2 MU) was used for all solution preparations.

Synthesis of the high-entropy double perovskite hollow nanofibers

Typically, 1.5 mmol $La(NO_3)_3·6H_2O$, 1.5 mmol $(CH_3COO)_2Sr$, 0.45 mmol $Fe(NO_3)_2·6H_2O$, 1.2 mmol $Co(NO_3)_2·6H_2O$, 0.45 mmol $Ni(NO_3)_2·6H_2O$, 0.45 mmol $(CH_3COO)_2Mn$, 0.45 mmol $Cu(NO_3)_2·6H_2O$ and 2 g PVP were sequentially dissolved in the mixed solution (10 g DMF and 10 g ethanol) under magnetic stirring for 5 h to obtain a homogeneous solution with the mass ratio of 30 wt% (mental salts to PVP) at room temperature. Then, the prepared LaSrMnFeCoNiCu salts/PVP precursor solution was directly injected into a 10 mL syringe equipped with a 22 gauge stainless steel needle at the tip. Afterwards, the LSMFCNC salts/PVP nanofibrous membranes were obtained through the electrospinning method. The electrospinning parameters were shown as follows. The anode voltage was 16 kV and the distance between the needle tip and tin foil collector was 15 cm with the temperature and the humidity set at 25 ^oC and 30%, respectively. The flow rate and electrospinning period were 0.3 mL h^{-1} and 12 h, respectively. The obtained precursor membrane was placed into a home-built chemical vapor deposition (CVD) system and then was oxidized at setting temperature for 3 h in air. After the CVD system was cooled down to the room temperature in air, the ($La_{0.5}Sr_{0.5}Mn_{0.15}Fe_{0.15}Co_{0.4}Ni_{0.15}Cu_{0.15}O_3$) LSMFCNC high-entropy perovskite oxide hollow nanofibers were obtained. The control samples were prepared using metal salts with the total amount of 6 mmol and treated with similar process with that of LSMFCNC.

Materials characterizations

The field emission scanning electron microscopy (FE-SEM) images were characterized via a HITACHI S-4800 (Japan) at an acceleration voltage of 3 kV. Transmission electron microscopy (TEM) images were taken using a JSM-2100 (JEOL, Japan) at an acceleration voltage of 200 kV. High-angle annular dark field scanning transmission electron microscopy (HAADF-STEM) images and STEM mapping were recorded using a STEM (FEI Tecnai F20, USA) at an acceleration voltage of 300 kV. The metal contents of catalysis were analyzed by Inductively Coupled Plasma Optical Emission Spectrometer (ICP-OES, PerkinElmer 8300). X-ray diffraction (XRD) patterns were analyzed using a Bruker AXS D8 DISCOVER X-ray diffractometer with Cu K_α radiation (k = 1.5406 Å) at a scanning rate of 0.02^o (2θ) in the 2θ range of 10-90°. X-ray photoelectron spectroscopy (XPS, Kratos Axis supra) analyses were acquired with an aluminum (mono) K_α source (1486.6 eV). The Al K_α source was operated at 15 kV and 10 mA.

Electrode preparation

A glass carbon electrode (GCE, with diameter of 3 mm) was used as the working electrode. The working electrodes were prepared according to the following procedure. Firstly, 3 mg catalysts were dispersed in 1 mL isopropanol. Then 25mL of 0.2 wt% Nafion was added into the suspension, then 5mL catalyst suspension was dropped onto the GCE and dried in air naturally.

Electrochemical measurements

The electrochemical measurements were performed on CHI660D electrochemical work station (CH Instruments, Inc., China) with a standard three-electrode system in 1 M KOH at room temperature. The GCE with as-synthesized catalysts was used as the working electrode, carbon rod and a saturated calomel electrode (SCE) served as the counter electrode and the reference electrode. The potential reported in this study were calibrated and converted to the reversible hydrogen electrode (RHE) by the equation E(RHE)= E(SCE)+ 0.244 + 0.059 × pH. The OER activity was evaluated by linear sweep voltammetry (LSV) with a sweep rate of 5 mV s^{-1} and the OER tests were performed between 0 and 0.8 V. The long-term durability was evaluated by chronoamperometry and Cyclic voltammetry (CV) measurements. Electrochemical impedance spectroscopy (EIS) was tested at open circuit voltage from 0.01 Hz to 100 kHz with an amplitude of 5 mV. CV curves were collected at different scan rates to measure the electrochemically active surface area (ECSA). For the calibration of reference electrodes, the new standard calomel electrode and the working calomel electrode were used as the count electrode and working electrode in saturated KCl solution to measure the potential changes before electrochemical measurement. All the reference electrodes were calibrated at each electrochemical measurement.

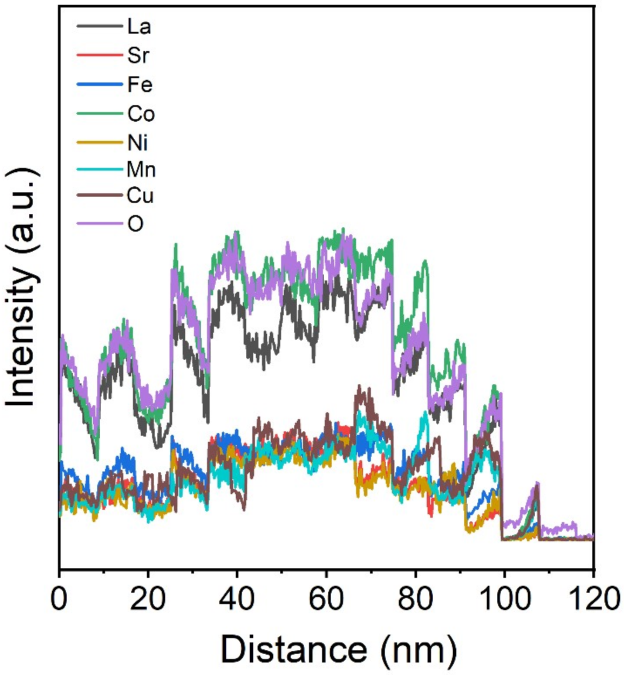

Figure S1. Line-scan EDX spectra of the typical LSMFCNC hollow nanofibers.

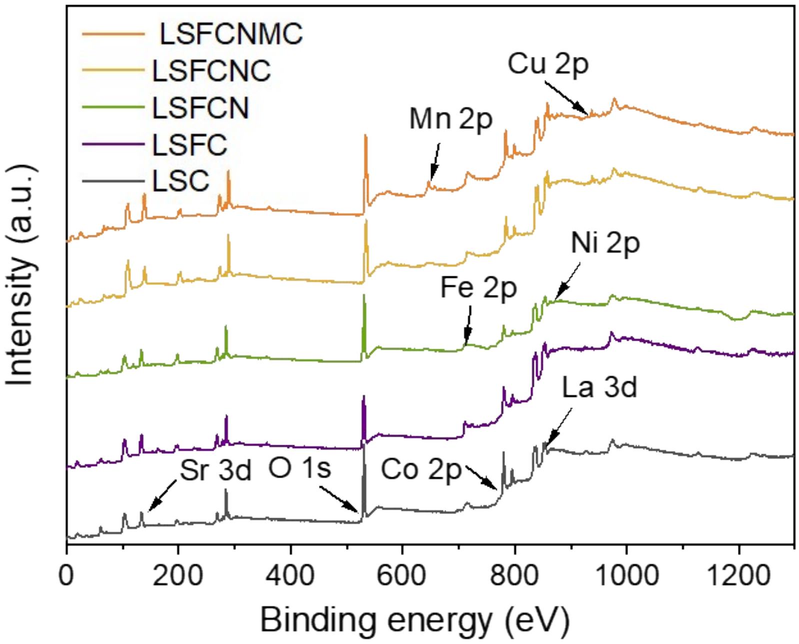

Figure S2. XPS survey spectrum of the as-prepared samples.

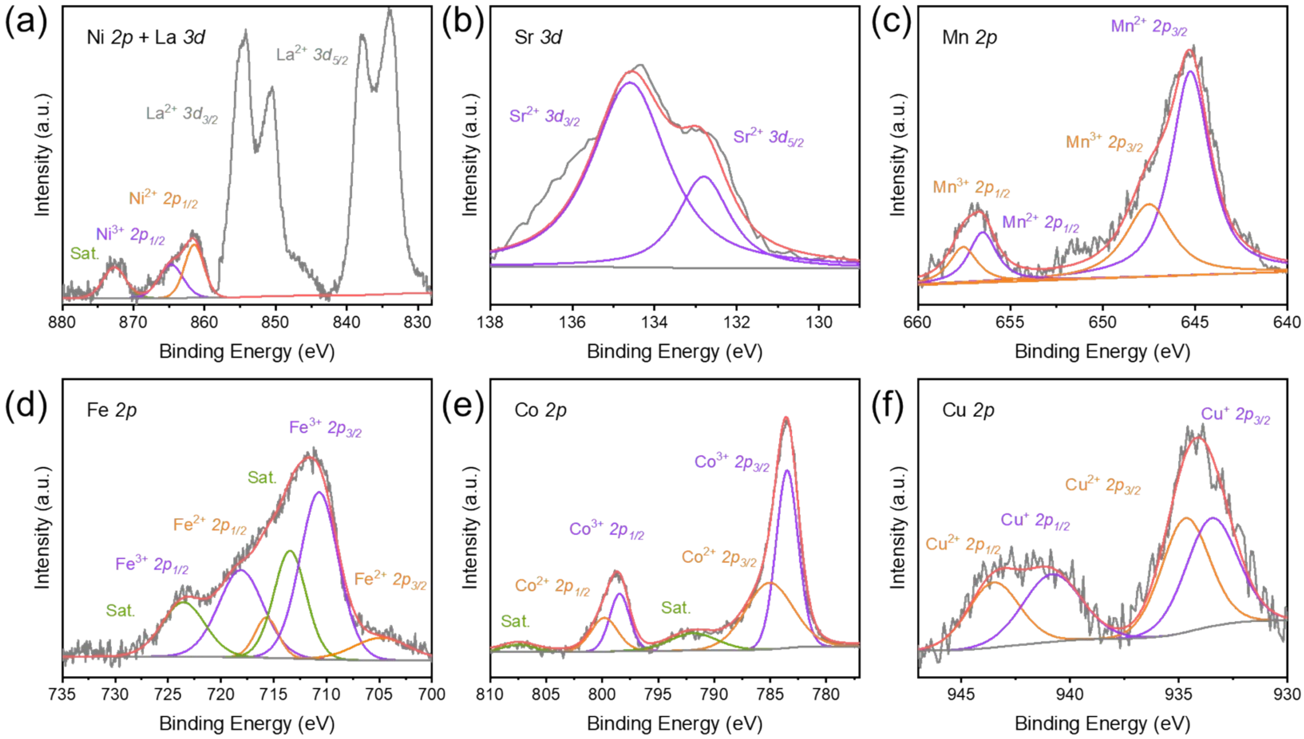

Figure S3. High-resolution XPS spectra of the as-prepared LSMFCNC: (a) Ni 2p and La 3d, (b) Sr 3d, (c) Mn 2p, (d) Fe 2p, (e) Co 2p and (f) Cu 2p.

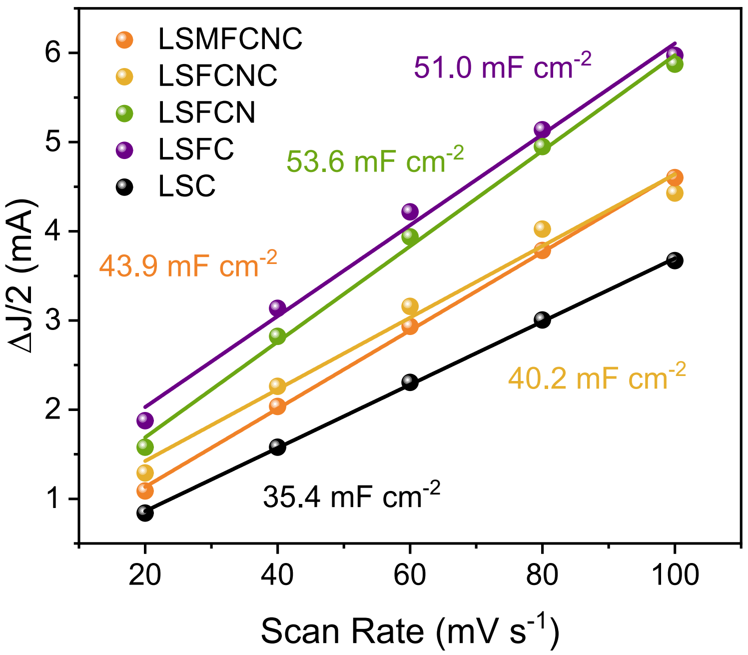

Figure S4. Double-layer capacitance per geometric area (C_{dl}) of the as-prepared samples supported on GCE.

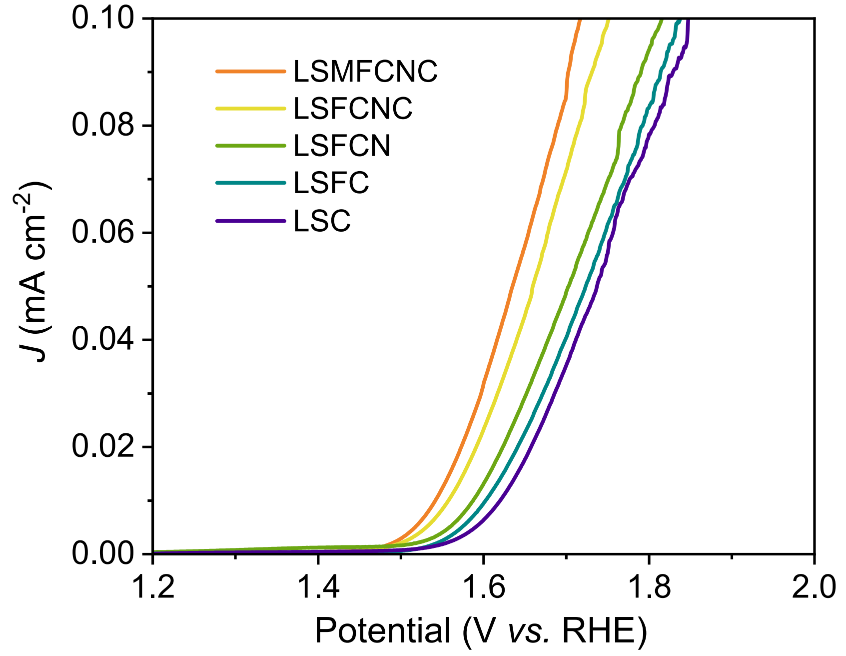

Figure S5. The ECSA-normalized LSV curves of the as-prepared samples.

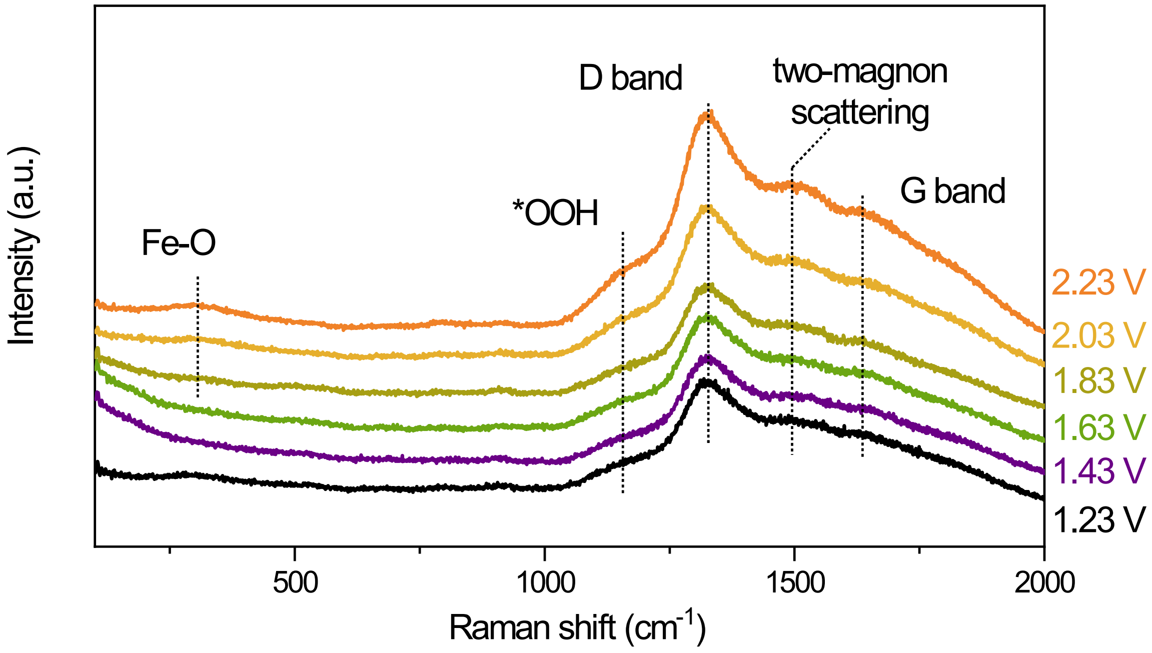

Figure S6. The operando electrochemical Raman spectra of LSFCN.

Table S1. The atomic percentages of La, Sr, Mn, Fe, Co, Ni, and Cu in LSMFCNC measured by ICP-OES and EDS.

LSMFCNC	La	Sr	Mn	Fe	Co	Ni	Cu
ICP-OES	26.1	27.0	7.5	6.9	18.9	7.1	6.5
EDS	24.6	20.5	7.8	8.2	22.4	8.7	7.7

Table S2. Summarized overpotentials at 10 mA cm^{-2} (η_{10}) and Tafel slopes of electrocatalysts for OER in 1.0 M KOH.

Electrocatalysts	η_{10}(mV)	Ref
LSMFCNC	309	This work
$La(CrMnFeCo_2Ni)O_3$	325	1
$LaFe_xNi_{1-x}O_3$	302	2
$FeOOH-LaNiO_3$	350	3
Si-SrCoO	417	4
$K_{1-x}Na_x(MgMnFeCoNi)F_3$	369	5
$CoSn(OH)_6$	350	6
$La_{1.8}CoMnO_{6-\delta}$	350	7
$Sr_{0.9}Co_{0.5}Fe_{0.35}Ni_{0.15}O_{3-\delta}$	282	8
$LaNiO_{3-\delta}$	309	9
$La_{0.2}Sr_{0.8}CoO_3$	360	10
$Pr_{0.5}Sr_{0.5}Co_{0.8}Fe_{0.2}O_{3-\delta}$	320	11
$BaFe_{0.8}Co_{0.2}O_3$	400	12
$SrLaCoO_{4-x}Cl_x$	370	13
$PrBa_{0.5}Sr_{0.5}Co_{1.5}Fe_{0.5}O_{5+\delta}$	313	14
$GdBaCo_{2-x}Fe_xO_{5+\delta}$	298	15

References

1. T. Nguyen, Y. Liao, C. Lin, Y. Su and J. Ting, *Adv. Funct. Mater.*, 2021, **31**, 2101632.
2. H. Wang, J. Wang, Y. Pi, Q. Shao and X. Huang, *Angew. Chem., Int. Ed.*, 2019, **58**, 2316–2320.
3. J. Zhao, C. Li, Z. Shi, J. Guan and G. Li, *Research*, 2020, 6961578.
4. Y. Pan, X. Xu, Y. Zhong, L. Ge, Y. Chen, J. P. Marcel Veder, D. Guan, R. O'Hayre, M. Li, G. Wang, H. Wang, W. Zhou and Z. Shao, *Nat. Commun.*, 2020, **11** , 1–10.
5. T. Wang, H. Chen, Z. Yang, J. Liang and S. Dai, *J. Am. Chem. Soc.*, 2020, **142**, 4550−4554.
6. M. Narahara, S. Y. Lee, K. Sasaki, K. Fukushima, K. Tanaka, S. Chae, X. Hu, G. Panomsuwan and T. Ishizaki, *Sustainable Energy Fuels*, 2023, **7**, 2582.
7. S. Li, J. Zheng and D. Yan, *Inorg. Chem.*, 2023, **62**, 11009−11015.
8. T. Chen, S. Sun, Y. He, H. Leng, C. Sun and C. Wu, *Journal of Alloys and Compounds*, 2023, **960** , 170974.
9. Y. Tang, C. Wu, Q. Zhang, H. Zhong, A. Zou, J. Li, Y. Ma, H. An, Z. Yu, S. Xi, J. Xue, X. Wang and J. Wu, *Angew. Chem. Int. Ed.*, 2023, e202309107.
10. R. Hu, L. Wei, J. Xian, G. Fang, Z. Wu, M. Fan, J. Guo, Q. Li, K. Liu, H. Jiang, W. Xu, J. Wan and Y. Yao, *Acta Phys. -Chim. Sin.*, 2023, **39**, 2212025.
11. S. Wu, J. Li, J. Hu, Y. Huang, H. Xu and K. Tang, *ACS Appl. Energy Mater.*, 2023, **6**, 6289−6298.
12. K. Iwase, M. Ohtaka and I. Honma, *Chem. Mater.*, 2023, **35**, 2773−2781.
13. S. Li, B. Zhang, Y. Li and D. Yan, *Inorg. Chem.*, 2023, **62**, 11233−11239.
14. Y. Zhu, L. Zhang, B. Zhao, H. Chen, X. Liu, R. Zhao, X. Wang, J. Liu, Y. Chen and M. Liu, *Adv. Funct. Mater.*, 2019, **29**, 1901783.
15. Y. Shuai, S. Liu, Y. Wang, W. Zhou, X. Qi and Y. Liu, *Catalysis Communications*, 2023, **174** , 106854.